

PAPER • OPEN ACCESS

Investigation of magnetization reversal processes in $\text{Sm}(\text{Co}, \text{Fe}, \text{Cu}, \text{Zr})_{7.5}$ magnets

To cite this article: A N Urzhumtsev *et al* 2019 *J. Phys.: Conf. Ser.* **1389** 012115

View the [article online](#) for updates and enhancements.



IOP | ebooks™

Bringing together innovative digital publishing with leading authors from the global scientific community.

Start exploring the collection—download the first chapter of every title for free.

Investigation of magnetization reversal processes in $\text{Sm}(\text{Co}, \text{Fe}, \text{Cu}, \text{Zr})_{7.5}$ magnets

A N Urzhumtsev¹, S V Andreev¹, M K Sharin², V N Moskaev² and A S Volegov^{1,3}

¹UrFU, Institute of Natural Sciences and Mathematics, 620000 Yekaterinburg, Russia

²LLC POZ - Progress, 624092 Verkhnyaya Pyshma, Russia

³IMP UB RAS, 620108 Yekaterinburg, Russia

E-mail: andrei.urzhumtsev@urfu.ru

Abstract. The processes of magnetization reversal in isotropic and anisotropic commercial permanent magnets $\text{Sm}(\text{Co}, \text{Fe}, \text{Cu}, \text{Zr})_{7.5}$ were investigated. Features of magnetization reversal process in both textured and isotropic magnets were analyzed with $\delta M(H)$ plots, magnetic susceptibility and initial magnetization curves. The magnetization reversal of $\text{Sm}(\text{Co}, \text{Fe}, \text{Cu}, \text{Zr})_{7.5}$ magnets is more complicated than that described in the coercivity model based on the domain walls pinning.

1. Introduction

Permanent magnets based on $\text{Sm}_2\text{Co}_{17}$ and SmCo_5 compounds are widely used in the aerospace and defense industries as part of gyroscopes and accelerometers, as well as microwave signal emitters, sensors and actuators. This is only a small part of examples of applications where permanent magnets with a high value of the maximum energy product $(BH)_{\text{max}}$ and low temperature coefficient of coercivity and remanence are required. Standard commercial magnets of these types meet the specified requirements in the temperature range -60 to $+300$ °C [1]. Currently, the $\text{Sm}(\text{Co}, \text{Fe}, \text{Cu}, \text{Zr})_z$ ($z = 7.0 - 8.5$) (with the rhombohedral structure of $\text{Th}_2\text{Zn}_{17}$ type) magnets again attract considerable attention due to the further increase of working temperature and maximal energy product [2].

With the high demand for the permanent magnets of the $\text{Sm}(\text{Co}, \text{Fe}, \text{Cu}, \text{Zr})_z$ system questions about the processes of magnetic reversal in them are still open. Studies of the magnetization reversal process are mainly carried out on rapidly quenched alloys [1-4].

The high coercivity of the $\text{Sm}(\text{Co}, \text{Fe}, \text{Cu}, \text{Zr})_z$ magnets is due to the coexistence of the matrix of cells $\text{Sm}_2(\text{Co}, \text{Fe})_{17}$ (2:17) with rhombohedral microstructure having a characteristic size of about 20 – 100 nm are surrounded by the $\text{Sm}(\text{Co}, \text{Cu})_5$ (1:5) phase with a thickness of about 2 – 10 nm, enriched with copper and a lamellar phase enriched with Zr with a thickness of 1 – 2 nm [1, 2, 4]. It is believed [1-5] that the coercivity mechanism of the $\text{Sm}(\text{Co}, \text{Fe}, \text{Cu}, \text{Zr})_z$ magnets is associated with the pinning of the domain walls in the phase boundary between 1:5 and 2:17 phases. The coercivity is determined by the difference of the domain wall energy $\Delta\gamma$ (1) between phases 2:17 and 1:5:

$$\Delta\gamma = (K_1^{2:17} A_1^{2:17})^{1/2} - (K_1^{1:5} A_1^{1:5})^{1/2} \quad (1)$$

where K_1 is the first anisotropy constant and A_1 is the exchange stiffness [3].

The applicable of the pinning model was demonstrated in describing the temperature dependence of coercivity. The abnormal temperature dependence of the coercivity of the magnets was explained in



terms of a specific mechanism for fixing domain walls, described as the transition from the repulsive fixation ($K_1^{1:5} > K_1^{2:17}$) to the attracting fixture ($K_1^{1:5} < K_1^{2:17}$) which is determined by the composition of the magnets. In addition, it can be assumed that the nucleation mechanism is active only in a relatively narrow temperature interval between the Curie temperature of 1:5 and the temperature of the matrix phase 2:17 [5].

Information about mechanisms of coercivity and interaction in the sample can be obtained from macroscopic magnetic measurements. One of the widely used techniques for polycrystalline samples is an investigation of isothermal magnetization $M_R(H)$ and DC demagnetization $M_D(H)$ remanences as the functions of applied magnetic field H [6].

In accordance with the Stoner-Wolfart model for an isotropic ensemble of single-domain noninteracting particles, the following relationship holds:

$$M_D(H) = M_{R(H_{max})} - 2M_R(H) \quad (2)$$

The next step was made by Kelly et al. with introducing the following expression:

$$\delta m(H) = m_d(H) - [1 - 2m_r(H)] \quad (3)$$

It is believed that the positive value of $\delta m(H)$ is due to intergrain exchange coupling of ferromagnetic type while the negative value of $\delta m(H)$ is the result of dipole–dipole coupling [7-14].

Another method of investigating the processes of magnetization reversal is to investigate the dependence of total or irreversible magnetic susceptibility. Thus, in papers [11-14] have investigated the dependencies of M_{rev} vs. M_{irr} . It was concluded that the mechanism of the high coercive state of Sm(Co, Fe, Cu, Zr)_{7.5} rapidly quenched alloys is the pinning of the domain walls.

The purpose of the paper is to demonstrate that the magnetization reversal processes of commercially available Sm-Co magnets cannot be explained only by the domain wall pinning and required a comprehensive model description.

2. Experiments

Samples of textured and isotropic commercial magnets Sm(Co, Fe, Cu, Zr)_{7.5} were investigated. The alloy with the composition Sm_{25.60}Co_{49.93}Fe_{15.56}Cu_{5.91}Zr_{3.00} was synthesized by the induction melting in argon. After alloying the ingot was crushed and milled. Powder was pressed in applied magnetic field (textured magnet) and without magnetic field (isotropic magnet). The sintering process was carried out for 5 min at 1090 °C in a vacuum and for 30 min at 1088 °C in argon. Solid state treatment was carried out for 6 hours at 1060 °C with subsequent quenching to room temperature with argon stream. The next step was the exposure at 750 °C for 12 hours after which magnets were cooling down to 330 °C for 8 hours.

Magnetic measurements were carried out in magnetic field up to 90 kOe in the temperature range of 2 – 400 K using the PPMS DynaCool and MPMS-XL-7 EC Quantum Design measurement systems.

3. Results and discussions

Figure 1 shows the magnetization and demagnetization curves for the textured and isotropic Sm₂Co₁₇ magnets at a temperature $T = 300$ K.

From figure 1 it follows that the shape of the magnetization curve for a textured magnet is more complicated than it is interpreted in the classical concepts of the magnetization process by means of the pinning mechanism [2, 8]. There is inflection of the magnetization curve at $H \approx 10$ kOe. The inflection corresponds to the movement of domain walls in some grains. The presence of soft magnetic phase is eliminated considering almost rectangular shape of major hysteresis curve.

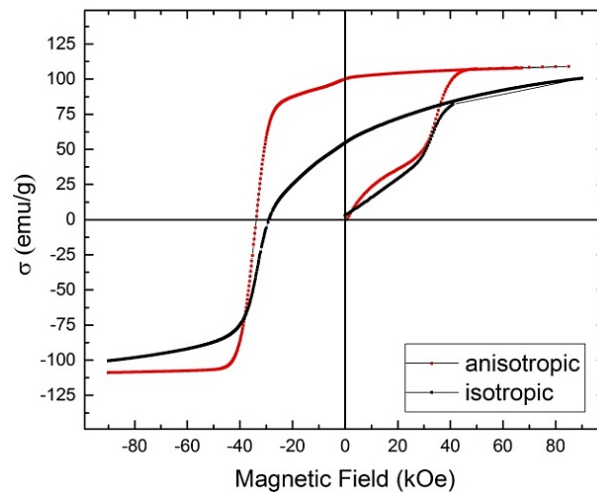


Figure 1. Magnetization and demagnetization curves of $\text{Sm}(\text{Co}, \text{Fe}, \text{Cu}, \text{Zr})_{7.5}$ magnets.

Similar effects were observed on the initial magnetization curves of sintered materials $\text{Nd}_2\text{Fe}_{14}\text{B}$ and SmCo_5 which seem almost magnetically soft [15]. The samples become almost completely magnetized in applied fields less than 1 kOe since the domain walls freely move inside the alloy grains. However, domain walls are effectively pinned by a high density of localized inhomogeneities at the grain boundaries or disappeared. This results in much higher coercive fields of tens of kOe.

Sub-microscopic information about coercive field mechanisms can sometimes be deduced from macroscopic magnetic measurements on thermally demagnetized samples by the Kelly's method [16]. Figure 2 shows the Kelly $[\delta m(H)]$ curves for $\text{Sm}_2\text{Co}_{17}$ magnets.

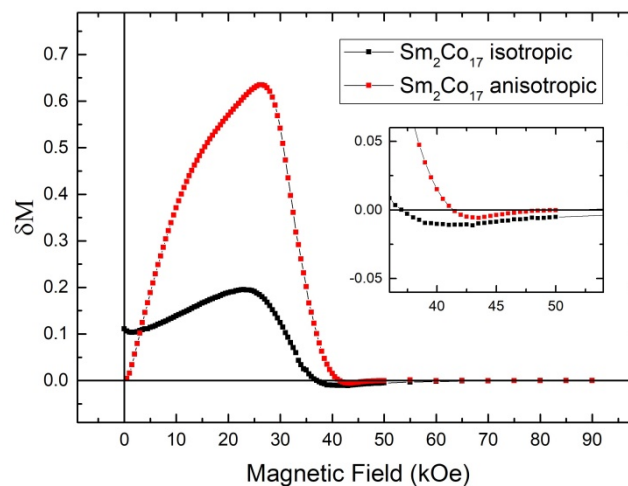


Figure 2. Kelly's plot for sintered permanent magnets $\text{Sm}(\text{Co}, \text{Fe}, \text{Cu}, \text{Zr})_{7.5}$.

From the Kelly's equation (3) it follows that a positive value of δM is observed in cases where the hard magnetic material is magnetized in smaller fields than it is demagnetized. This can be observed both in cases of a strong exchange coupling of the ferromagnetic type between the elements of the material, and in the case of a high-coercivity state due to nucleation [1, 8, 9, 15]. The δM deviation from zero in the whole range of fields is due to one of the following reasons: nonequivalence of the pinning locations of the domain walls in the material during magnetization and

demagnetization, multidomain initial state of some grains and significant intergranular exchange interaction [17]. The first assumption is very questionable instead of others.

Based on these dependencies and common opinion it could be indirectly conclude the intergrain exchange interaction significantly impacts on magnetization reversal processes. By the ratio of the sections under the curve, it can be interpreted that the exchange value in a textured magnet is significantly higher than in an isotropic magnet. Also this graph allows to consider the weakness of a magnetostatics interaction. From the other point of view nucleation leads to the positive value of δm . Because of inflection on magnetization curve we believe the reason for positive value of δm is nucleation type magnetic hysteresis.

Figures 3 (a) and (b) show total and irreversible magnetic susceptibility in the process of magnetizing (+H) and demagnetizing (−H). For the isotropic sample (figure 3 (a)), significant difference between total and irreversible magnetic susceptibility relates to reversible rotation of magnetization vector of grains easy magnetization axis of which oriented not along the magnetic field direction. The susceptibility of the samples during magnetization is higher. For the textured sample (figure 3 (b)), total and irreversible magnetic susceptibility almost the same and magnetization reversal is totally irreversible. Characteristic peak on the $\sigma(+H)$ and $\sigma_r(+H)$ curves in low magnetic field is related to the domain walls movement in multidomain particles.

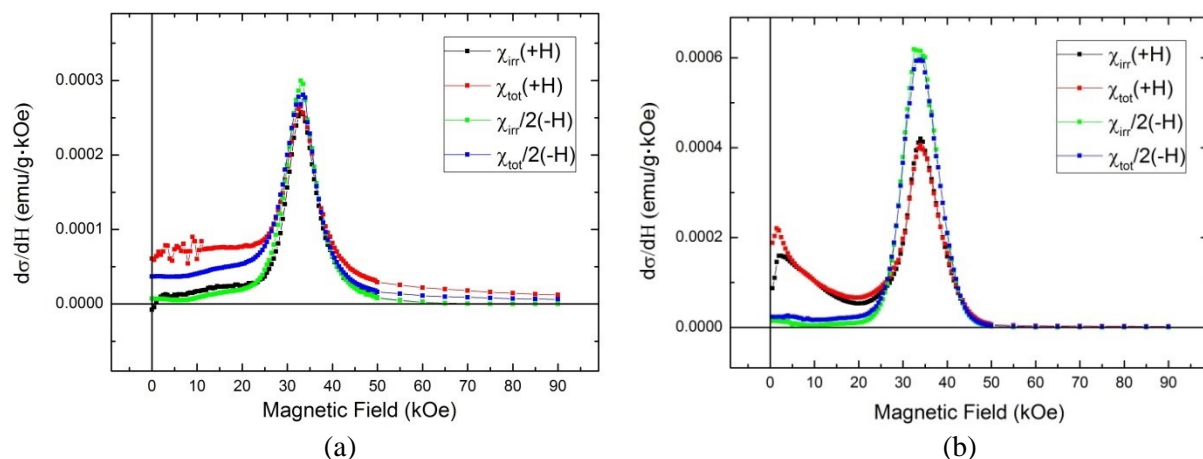


Figure 3. Derivative magnetization with the field applied and after the DC field is turned off (χ_{tot} and χ_{irr} correspondingly) for isotropic (a) and for textured (b) permanent magnet $\text{Sm}(\text{Co}, \text{Fe}, \text{Cu}, \text{Zr})_{7.5}$.

On the major demagnetization curves in figure 4 at a temperature of 2 K for an anisotropic magnet sample, Barkhausen jumps are observed meanwhile the same curve of isotropic sample is smooth. Apparently, some local demagnetization processes in anisotropic magnet creates heat wave which slightly changes hysteresis properties of neighboring grains. Magnetization of the grains changes and this process continues until the demagnetizing field decreases to the such value when heating become not enough to decrease switching field to reverse magnetization of next grains. The isotropic sample has the different microstructure with randomly oriented crystallites. It leads to broad distribution of coercivities and suppression of heat contact between grains with close values of coercivity. Similar magnetization jumps were observed on an isotropic rapidly quenched alloy of the NdFeB system [18].

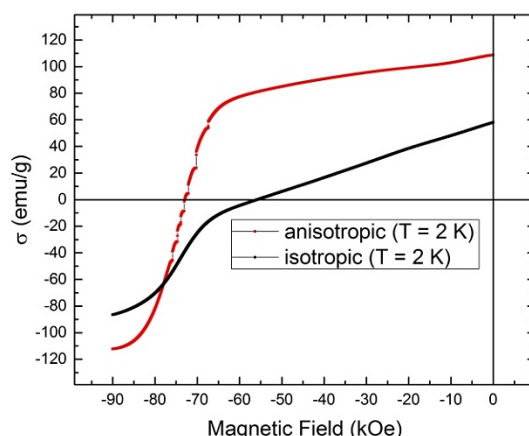


Figure 4. Demagnetization curves of permanent magnets $\text{Sm}(\text{Co}, \text{Fe}, \text{Cu}, \text{Zr})_{7.5}$ at 2 K.

4. Conclusion

The processes of magnetization reversal in permanent magnets $\text{Sm}(\text{Co}, \text{Fe}, \text{Cu}, \text{Zr})_{7.5}$ are more complex than pinning. The presence of multidomain grains in commercially available magnets was shown. The positive peak on $\delta m(H)$ plot was interpreted as a result of the presence of multidomain particles in magnets but not the intergrain exchange interaction.

Acknowledgements

The work was supported by Act 211 Government of the Russian Federation, contract № 02.A03.21.0006.

References

- [1] Gutfleisch O, Muller K-H, Khlopkov K, Wolf M, Yan A, Schäfer R, Gemming T and Schultz L 2006 *Acta Mater.* **54** 997–1008
- [2] Yan A, Bollero A, Müller K H and Gutfleisch O 2002 *Appl. Phys. Lett.* **80** 1243
- [3] Yan A, Gutfleisch O, Handstein A, Gemming T and Müller K-H 2003 *J. Appl. Phys.* **93** 7975
- [4] Yan A, Gutfleisch O, Gemming T and Müller K-H 2003 *Appl. Phys. Lett.* **83** 2208
- [5] Popov A G, Gaviko V S, Popov V V, Golovnia O A, Protasov A V, Gerasimov E G, Ogurtsov A V, Sharin M K and Gopalan R 2019 *JOM* **71** 559–66
- [6] Gaunt P, Hadjipanayis G and Ng D 1986 *JMMM* **54-57** 841–2
- [7] Chen R J, Wang J Z, Zhang H W, Shen B G and Yan A 2007 *J. Phys. D: Appl. Phys.* **40** 4391–5
- [8] Bolyachkin A S, Volegov A S and Kudrevatykh N V 2015 *JMMM* **378** 362–6
- [9] Gao R W, Zhang D H, Li W, Li X M and Zhang J C 2000 *JMMM* **208** 239–43
- [10] Ma Z, Zhang T and Jiang C 2015 *RSC Adv.* **5** 89128
- [11] Huang M Q, Turgut Z, Smith B R, Chen Z M, Ma B M, Chu S Y, Laughlin D E, Horwath J C and Fingers R T 2004 *IEEE Trans. Magn.* **40** 2934–6
- [12] Crew D C, Woodward R C and Street R 1999 *J. Appl. Phys.* **85** 5675–7
- [13] Rong C-B, Chen R-J, Zhang H-W, Zhang J, Zhang S Y and Shen B G 2004 *J. Phys. D: Appl. Phys.* **37** 3285–9
- [14] Rong C-B, Zhang H-W, Shen B-G and Liu J P 2006 *Appl. Phys. Lett.* **88** 042504
- [15] Buschow K H J 2003 *Physics of Magnetism and Magnetic Materials* ed. K H J Buschow and F R de Boer (New York: Kluwer Academic/Plenum Publishers)
- [16] Kelly P E, O'Grady K, Mayo P I and Chantrell R W 1989 *IEEE Trans. Magn.* **25** 3881–3
- [17] Fearon M, Chantrell R W and Wohlfarth E P 1990 *JMMM* **86** 197–206
- [18] Neznakhin D S, Bolyachkin A S, Volegov A S, Markin P E, Andreev S V and Kudrevatykh N V 2015 *JMMM* **377** 477–9.